Supporting Information

Conjugation-Break Spacers in Semiconducting Polymers: Impact on Polymer Processability and Charge Transport Properties

Yan Zhao,[†] *Xikang Zhao,*[†] *Yaping Zang,*[‡] *Chong-an Di,*[‡] *Ying Diao,*[§] *and Jianguo Mei**[,†,∥]

[†]Department of Chemistry, Purdue University, 560 Oval Drive, West Lafayette, Indiana 47907, United States

[‡]Key Laboratory of Organic Solids, Institute of Chemistry, Chinese Academy of Sciences, Beijing 100190, China

[§]Department of Chemical & Biomolecular Engineering, University of Illinois at Urbana−Champaign, 600 South Mathews Avenue, Urbana, Illinois 61801, United States

[∥]Birck Nanotechnology Center, Purdue University, 1205 W State St., West Lafayette, Indiana 47906, United States

Downloaded from pubs.acs.org/mamobx/article-supplement/1550151/pdf/ma5b00194_si_001/ by PURDUE UNIV user on 28 October 2026

Table of Contents **Page number**

Materials and synthesis S2-S3
Devices fabrication and characterization methods S4
NMR, GPC, TGA and DSC characterizations S5-S7
Electrical characterization of OFETs S8-S11
AFM images and GIXRD patterns S12-S13

Materials and characterizations

All reagents and starting materials were purchased from Sigma Aldrich and used without further purification, unless otherwise noted. ^{1}H and ^{13}C NMR spectra were recorded using Varian Inova 300 in deuterated chloroform at 293 K. Size exclusion chromatography (SEC) was performed in trichlorobenzene solution at 180 °C with EcoSEC HT GPC System (Tosoh Bioscience LLC) and the molecular weights calculated using a calibration curve based on polystyrene standards. Thermal gravimetric analyses (TGA) were performed using a Mettler TOLEDO TGA/SDTA851e at a heating rate of 10 °C min^{-1} under a nitrogen flow (20 mL/min). Differential scanning calorimetry (DSC) measurements were acquired using a TA Q1000 calorimeter. The results shown are for the final sample heating at a rate of 1°C/min. An indium standard was used to calibrate the instrument and nitrogen was used as the purge gas. UV-Vis-NIR spectra were recorded on an HP 8453 UV-visible spectrophotometer (400-1100 nm). 2D-GIXRD images were collected in reflection mode with a planar area detector in a He atmosphere at beamline 11-3 of the Stanford Synchrotron Radiation Lightsource. The sample-detector distance was nominally set to 400 mm, and the incidence angle was 0.12 degrees; the X-ray wavelength was 0.9758 Angstroms. Slits were set to 150 µm and 50 µm in the horizontal and vertical directions, respectively. GIXRD images were calibrated and analyzed using WxDiff software provided by Stefan Mannsfeld (Adv. Mater. 2011, 23, 127). For details about the sample chamber, please see (Adv. Funct. Mater.2010, 20, 3519).

Polymer synthesis

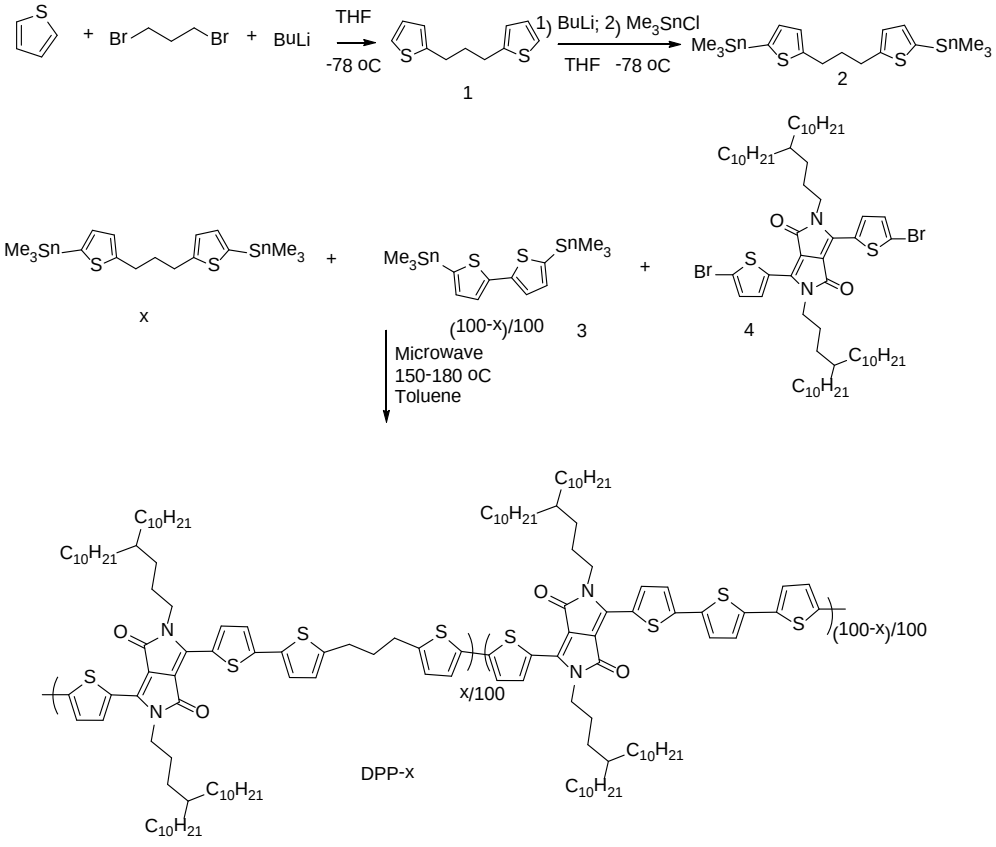

Downloaded from pubs.acs.org/mamobx/article-supplement/1550151/pdf/ma5b00194_si_001/ by PURDUE UNIV user on 28 October 2026

1,3-di(thiophen-2-yl)propane (1): To a cooled (−78 ºC) mixture of thiophene (8.13 g, 97 mmol) in anhydrous THF (50 mL), a solution of n-BuLi (73 mmol, 2.5 M) in n-hexane was added drop-wise. After stirring for 1 hour at 0 ºC, 1,6-dibromopropane (4.88g, 24 mmol) was injected through a septum. The mixture was slowly warmed up to room temperature by the removal of cooling bath. Water (250 mL) was added and the mixture was extracted with hexane (3 × 50 mL). The combined organic layers were dried over $MgSO_4$ and concentrated in vacuo. The crude product was purified by silica gel chromatography, eluting with hexane. The product was obtained as a colorless solid (3.2 g, 63%). ^{1}H NMR (300 MHz, Chloroform-*d*) δ 7.29 (dd, *J* = 5.1, 1.3 Hz, 2H), 7.10 (dd, *J* = 5.1, 3.4 Hz, 2H), 6.97 (d, *J* = 3.4, 1.3 Hz, 2H), 3.06 (t, *J* = 7.5 Hz, 4H), 2.33 − 2.16 (m, 2H). (Heterocycles, 1999, 51, 1059-1065.)

1,3-bis(5-(trimethylstannyl)thiophen-2-yl)propane (**2**): 1,3-di(thiophen-2-yl)propane (2.9 g) was dissolved in 60 mL of THF under argon, then the solution was cooled to −78 °C. n-BuLi (2.5 M, 12.8 mL, 32 mmol) was slowly added to the solution by syringe in 15 min. The reaction was maintained at −78 °C for 30 min, and warmed up to 20 °C for another 30 min. Then the solution was cooled to −78 °C again, and trimethyltin chloride (1 M, 32 mL, 32 mmol) was injected through a septum. The mixture was slowly warmed up to room temperature by the removal of cooling bath and stirred overnight. The solvent THF was evaporated, and the solid residue was redissolved in diethyl ether and washed with water. The organics were collected and dried over anhydrous Na_2SO_4 and activated carbon (essential to remove the color). After the solvent was removed via rotary evaporation, the crude product was purified by recrystallization from ethanol to give white solid (5.1 g, 68%). ^{1}H NMR (300 MHz, Chloroform-*d*) δ 7.04 (d, *J* = 3.2 Hz, 2H), 6.94 (d, *J* = 3.2 Hz, 2H), 2.96 (t, *J* = 7.5 Hz, 4H), 2.21 – 2.00 (m, 2H), 0.49 – 0.22 (m, 18H). ^{13}C NMR (75 MHz, CDCl3) δ 135.52, 134.97, 126.17, 125.80, 33.95, 29.60, -7.81.

General method for polymerization

To a microwave vessel (35 mL, CEM Discover Automatic Microwave Reactor) charged with a string bar were added 1,3-bis(5-(trimethylstannyl)thiophen-2-yl)propane, 5,5'-bis(trimethylstannyl)-2,2'-bithiophene (0.25 mmol), and 3,6-bis(5-bromothiophen-2-yl)-2,5-bis(4-decyltetradecyl)-2,5-dihydropyrrolo[3,4-c]pyrrole-1,4-dione in a desired ratio (x/100: (100-x)/100: 1, X =100, 70, 50, 30 and 0), anhydrous toluene (15 mL) was added under argon. The vessel was then sealed with a snap cap and purged with argon for 15-18 min. $Pd_2(dba)_3$ and $P(o\text{-}tyl)_3$ were added then under argon. The vessel was immediately transferred to the microwave chamber. The polymerization conditions are listed as follows: Power cycling mode; Power, 200 W; Power cycles, 100; Temperature, 150-180 °C; Heating, 120s; Cooling, 30s; Pressure, 150 psi; Stirring, high.). After the completion, the mixture was suspended into acetone and the precipitates were collected by a high quality glass thimble. The polymer was subject to purification by Soxhlet extraction with methanol, hexane and chloroform. The chloroform fraction was precipitated into methanol. The collected polymer was dried at 60 °C under vacuum with the yields in the range of 86-93%. The characterization data (NMR, TGA, DSC, GPC, UV-Vis) are given in the main text and in the supporting information.

Downloaded from pubs.acs.org/mamobx/article-supplement/1550151/pdf/ma5b00194_si_001/ by PURDUE UNIV user on 28 October 2026

Fabrication of FET devices.

A heavily n-doped Si wafer with a 300-nm SiO_2 surface layer (capacitance of 11 nF/cm^2) was employed as the substrate with Si wafer serving as the gate electrode and SiO_2 as the dielectric. The gold S/D electrodes were sputtered and patterned by photolithography technique. The device channel length was 30 μm, and the channel width was 1000 μm. For the octadecyltrichlorosilane (OTS) modification, the silicon wafer (with Au bottom contact) was first cleaned with hot piranha solution (H_2SO_4 (98%): H_2O_2 (30% water solution) = 7 : 3). It was then further subjected to sonication sequentially in water and acetone for 6 min each. After drying at an oven, the silicon wafer was then put in a petri dish with a small drop of OTS. The dish was then covered and heated in a vacuum oven at 120 °C for 3 h resulting in the formation of an OTS self-assembled monolayer on the surface. The OTS modified substrates were rinsed successively with hexane, ethanol, and chloroform, and dried by nitrogen. The semiconductor layer was deposited on the OTS-treated Si/SiO_2 substrates by spin coating, drop casting and melt processing. For spin coating, spin speed of 2000 r.p.m. was used to get a good polymer film. The concentrations of the solutions used for spin coating were 3 mg/mL for polymer DPP-0 and 10 mg/mL for other 4 polymers. The concentrations of the solutions used for drop casting is 1/3 of those for spin coating. For melt processed OFETs, a small amount of polymer was put on the glass or silicon substrates on a hot plate. After the polymer melted at proper temperature, the OTS modified silicon wafer was covered from top of the melted polymer. The silicon wafer was then pushed to one direction to obtain the polymer film.

Device characterization

Device characterization of the fabricated OFETs was carried out using Keithley 2400 in ambient air. The field-effect mobility was calculated in the saturation regime by using the equation $I_{DS} = (\mu WC_i/2L)(V_G - V_T)^2$, where I_{DS} is the drain–source current, μ is the field-effect mobility, W is the channel width, L is the channel length, C_i is the capacitance per unit area of the gate dielectric layer, V_G is the gate voltage, and V_T is the threshold voltage.

Downloaded from pubs.acs.org/mamobx/article-supplement/1550151/pdf/ma5b00194_si_001/ by PURDUE UNIV user on 28 October 2026

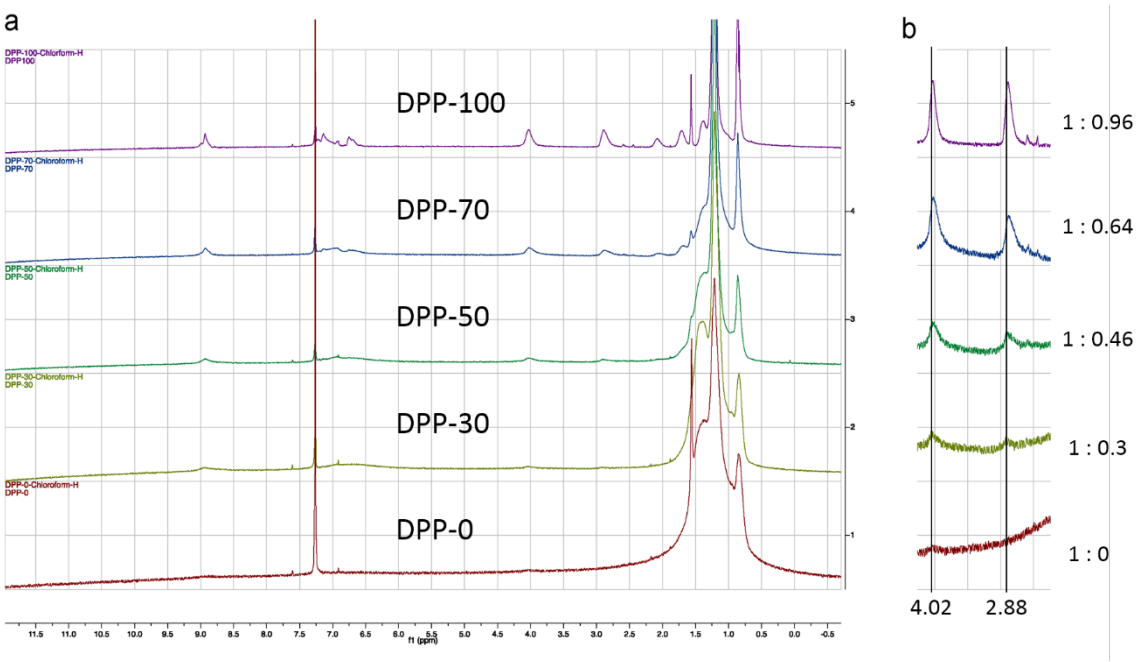

Fig. S1 (a) NMR spectra of DPP polymers. (b) Enlarged portion from 2.25 to 4.25 ppm.

Downloaded from pubs.acs.org/mamobx/article-supplement/1550151/pdf/ma5b00194_si_001/ by PURDUE UNIV user on 28 October 2026

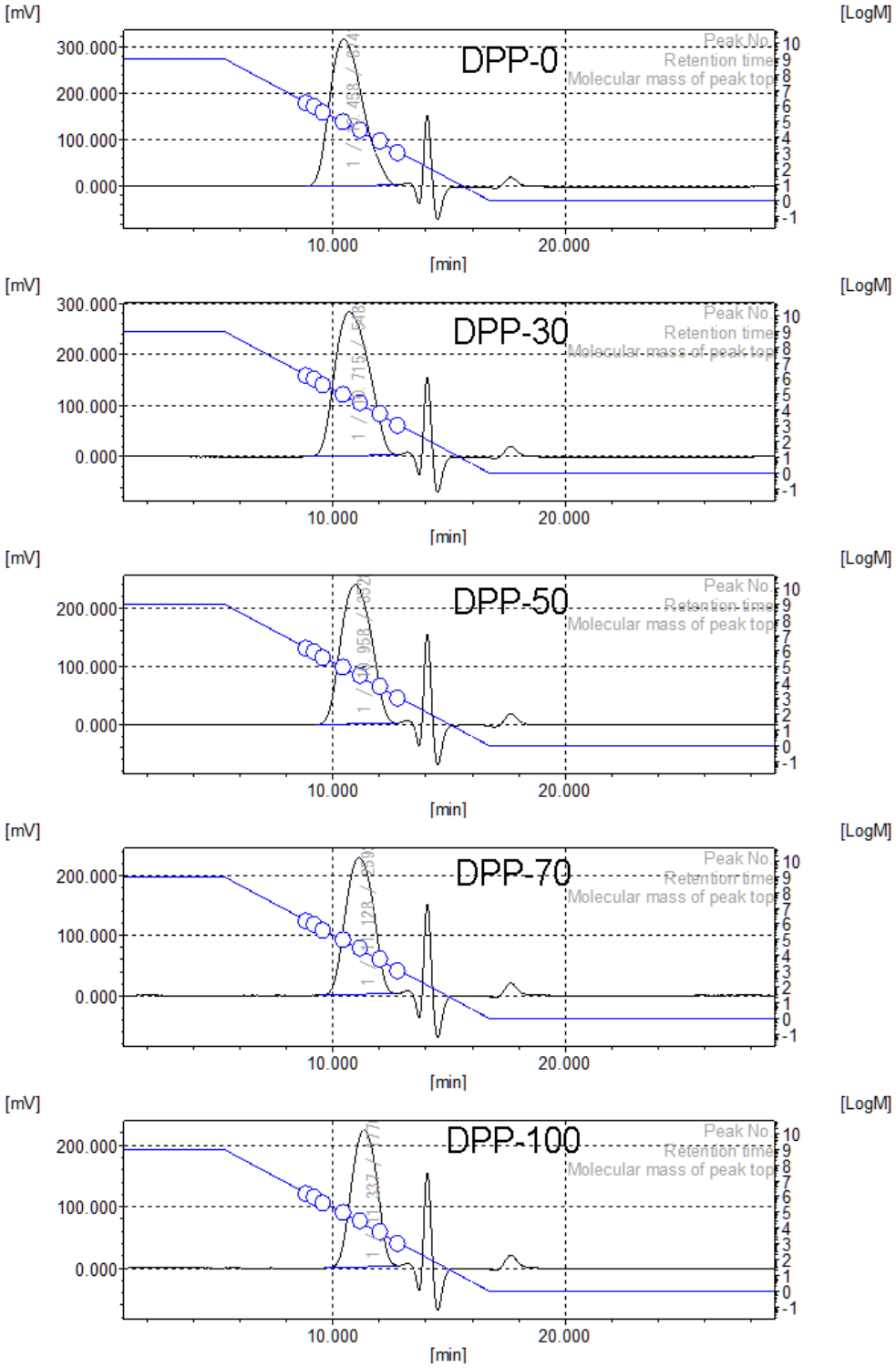

Fig. S2 GPC traces of DPP polymers (1,2,4-trichlorobenzene as the eluent at 180 °C). With increasing the CBS ratio, the GPC traces of DPP-x get sharper. Note: The molecular weights are estimated by using polystyrene as the standard. However, it may not be fair to directly compare the molecular weights of DPP polymers, as these polymers likely present different conformations ranged from random-coil to rigid-rod.

Downloaded from pubs.acs.org/mamobx/article-supplement/1550151/pdf/ma5b00194_si_001/ by PURDUE UNIV user on 28 October 2026

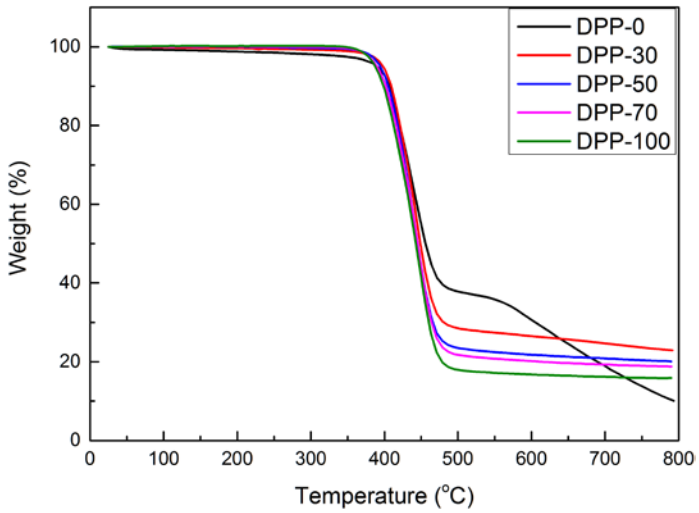

Fig. S3 Thermogravimetric analysis (TGA) curves of DPP polymers (10 °C/min under nitrogen atmosphere)

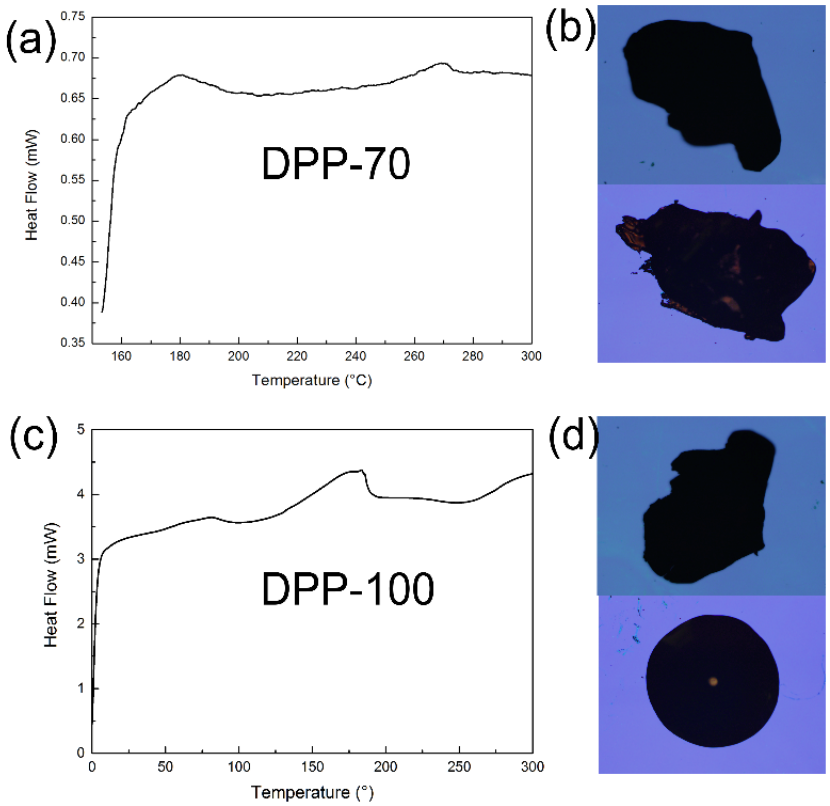

Fig. S4 (a) and (c) are differential scanning calorimetry (DSC) curves of DPP-70 and DPP-100 polymers, respectively (1 °C/min under nitrogen atmosphere). (b) and (d) are optical images of polymers before (top) and after (bottom) melt for DPP-70 and DPP-100, respectively. Note: 1) No noticeable thermal transition in the range of 100-350 °C was observed for DPP-0, -30 and -50. The thermal transitions in DPP-70 and DPP-100 were not reversible, and only appeared in the first circle. The melting behaviors can be observed visually on a hotplate when the samples were heated up to the 250 °C and 180 °C for DPP-70 and DPP-100, see (b) and (d).

Downloaded from pubs.acs.org/mamobx/article-supplement/1550151/pdf/ma5b00194_si_001/ by PURDUE UNIV user on 28 October 2026

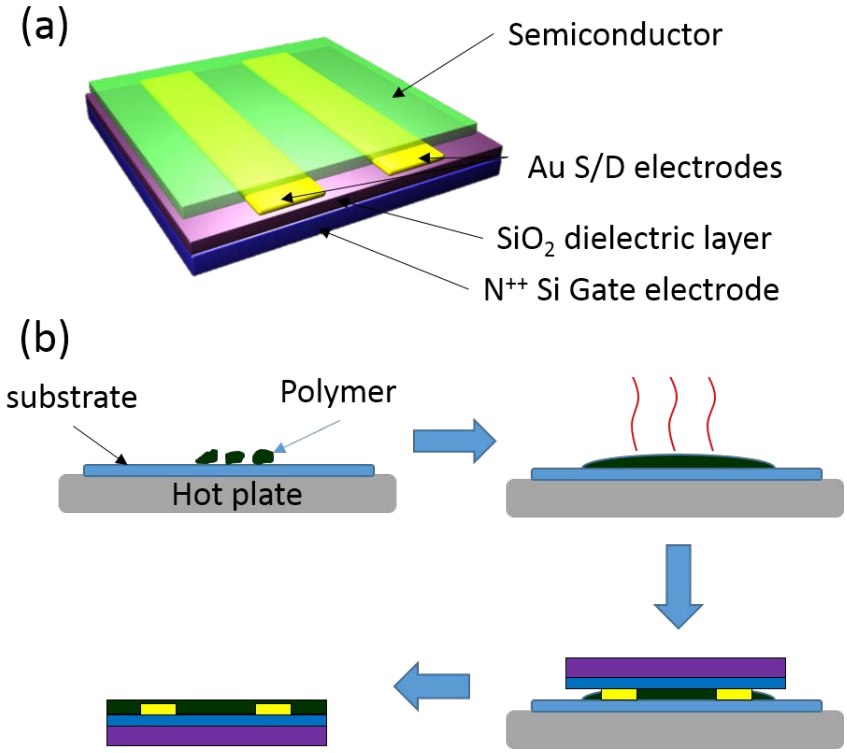

Fig. S5 (a) Schematic of the BGBC OFET device geometry in this work. (b) Schematic illustration of the melt process. See method section for details of the device fabrication.

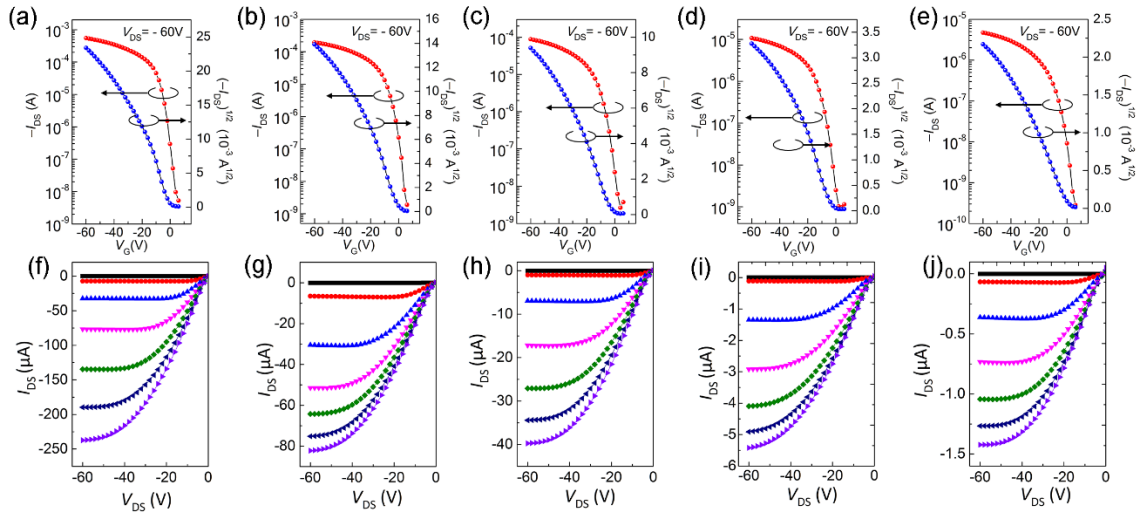

Fig. S6 Transfer and output characteristics of polymer OFETs fabricated by spin coating. (a), (b), (c), (d) and (e) are transfer characteristics for DPP-0, DPP-30, DPP-50, DPP-70 and DPP-100 OFETs, respectively. (f), (g), (h), (i) and (j) are output characteristics for DPP-0, DPP-30, DPP-50, DPP-70 and DPP-100 OFETs respectively. The V_G was set from 0 V to −60 V in steps of −10 V for all output testing.

Downloaded from pubs.acs.org/mamobx/article-supplement/1550151/pdf/ma5b00194_si_001/ by PURDUE UNIV user on 28 October 2026

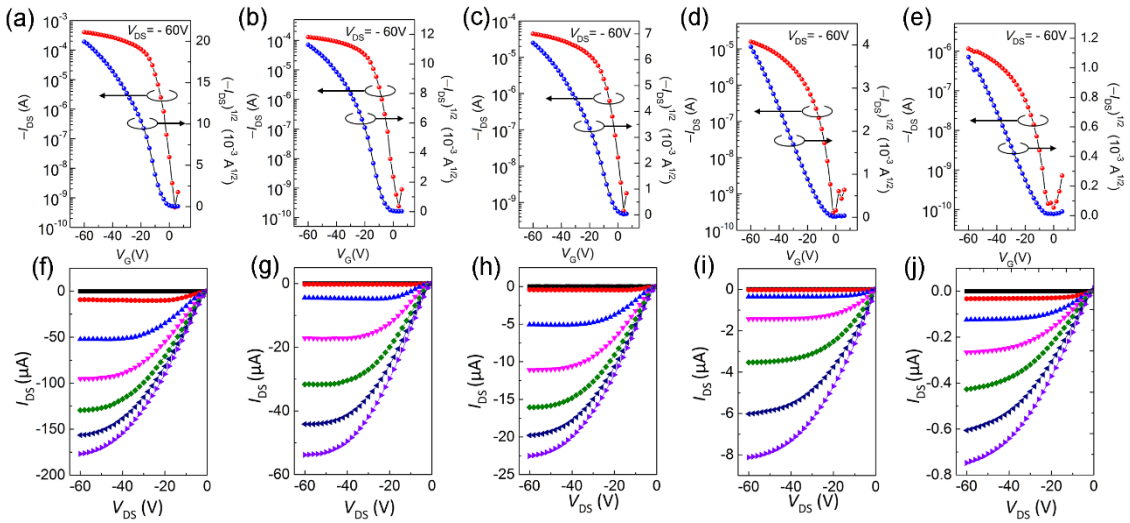

Fig. S7 Transfer and output characteristics of polymer OFETs fabricated by drop casting. (a), (b), (c), (d) and (e) are transfer characteristics for DPP-0, DPP-30, DPP-50, DPP-70 and DPP-100 OFETs respectively. (f), (g), (h), (i) and (j) are output characteristics for DPP-0, DPP-30, DPP-50, DPP-70 and DPP-100 OFETs respectively. The V_G was set from 0 V to −60 V in steps of −10 V for all output testing.

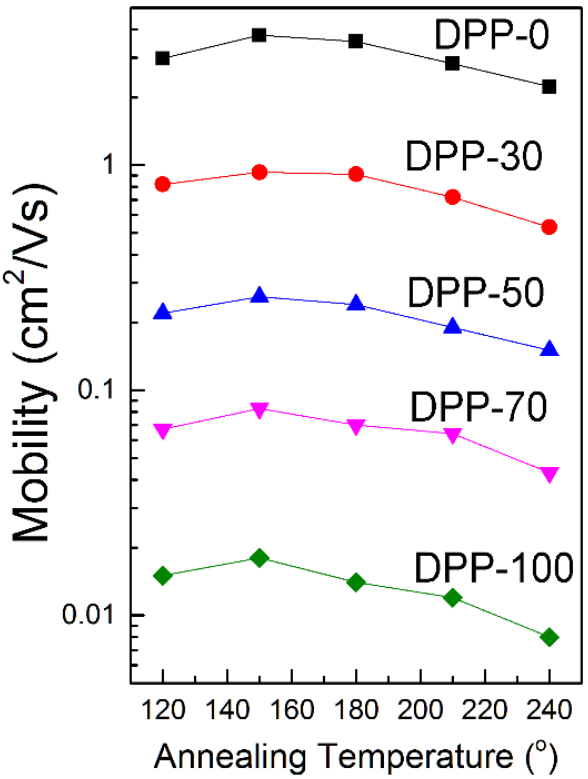

Fig. S8 Relationship between annealing temperature and mobility. The optimized annealing temperature is 150 °C for all polymers in this work.

Downloaded from pubs.acs.org/mamobx/article-supplement/1550151/pdf/ma5b00194_si_001/ by PURDUE UNIV user on 28 October 2026

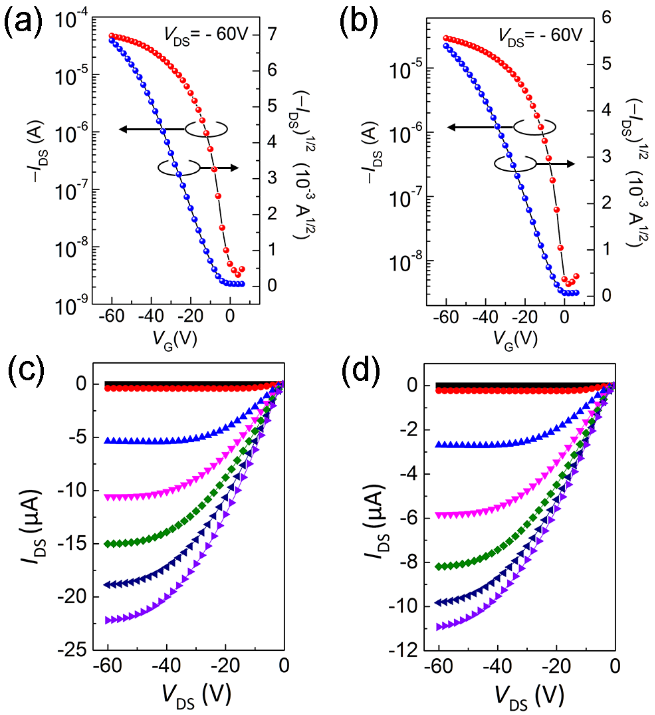

Fig. S9 (a) Transfer and (c) output characteristics of melt processed DPP-70 OFETs fabricated under protection of nitrogen. (b) Transfer and (d) output characteristics of melt processed DPP-70 OFETs fabricated in ambient air. The V_G was set from 0 V to −60 V in steps of −10 V for all output testing.

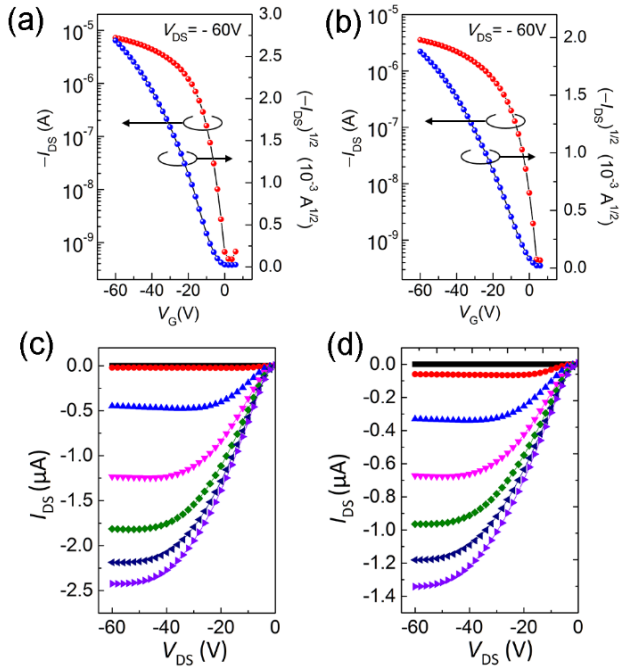

Fig. S10 (a) Transfer and c) output characteristics of melt processed DPP-100 OFETs fabricated under protection of nitrogen. (b) Transfer and (d) output characteristics of melt processed DPP-100 OFETs fabricated in ambient air. The V_G was set from 0 V to −60 V in steps of −10 V for all output testing.

Downloaded from pubs.acs.org/mamobx/article-supplement/1550151/pdf/ma5b00194_si_001/ by PURDUE UNIV user on 28 October 2026

Table S1 OFET results from Dr. Chongan Di's lab at Institute of Chemistry, Chinese Academy of Sciences

	μ_{max} (cm^2/Vs)	μ_{avg} (cm^2/Vs)	V_{Th} (V)	I_{on}/I_{off}
DPP-0	5.0	4.25	−3.0	~10^5
DPP-30	1.2	1.0	−1.9	~10^5
DPP-50	0.41	0.34	−2.2	~10^7
DPP-70	0.17	0.12	−1.8	~10^8
DPP-100	0.04	0.02	−4.2	~10^8

All OFETs were fabricated by spin coating. The annealing procdure was carried out in a vacuum oven at 150 °C. The devices were tested in ambient air with a Keithley 4200 semiconductor characterizatin system.

Table S2 OFET characteristics of with annealing procdure carried out in ambient air.

	μ_{max} (cm^2/Vs)	μ_{avg} (cm^2/Vs)	V_{Th} (V)	I_{on}/I_{off}
DPP-0	4.15	3.96	−4.6	~10^5
DPP-30	1.23	0.89	−5.7	~10^5
DPP-50	0.42	0.19	−5.4	~10^5
DPP-70	0.079	0.062	−5.9	~10^4
DPP-100	0.021	0.014	−7.1	~10^4

All OFETs were fabricated by drop casting. The annealing procdure was carried out on a hot plate at 150 °C in ambient air for 5 minutes.

Table S3 OFET characteristics of the melt processed devices in air without N_2 flow protection.

	μ_{max} (cm^2/Vs)	μ_{avg} (cm^2/Vs)	V_{Th} (V)	I_{on}/I_{off}
DPP-70	0.18	0.012	−4	~10^5
DPP-100	0.013	0.009	−4	~10^5

Table S4 OFETs characteristics of DPP polymers by using toluene as solvent.

	μ_{max} (cm^2/Vs)	μ_{avg} (cm^2/Vs)	V_{Th} (V)	I_{on}/I_{off}
DPP-0	0.94	0.78	−4.1	~10^5
DPP-30	0.34	0.21	−4.5	~10^5
DPP-50	0.096	0.073	−5.1	~10^5
DPP-70	0.046	0.035	−6.8	~10^4
DPP-100	0.025	0.014	−8.9	~10^4

Toluene was used as non-halogenated solvent to study the influence of CBSs to the processability of these polymers.The devices were fabricated by spin coating. For DPP-0, the solubility in toluene is very low (<1 mg/mL). Hence, the use of toluene as a processing solvent has the bigger impact on DPP-0 than on DPP-100.

Downloaded from pubs.acs.org/mamobx/article-supplement/1550151/pdf/ma5b00194_si_001/ by PURDUE UNIV user on 28 October 2026

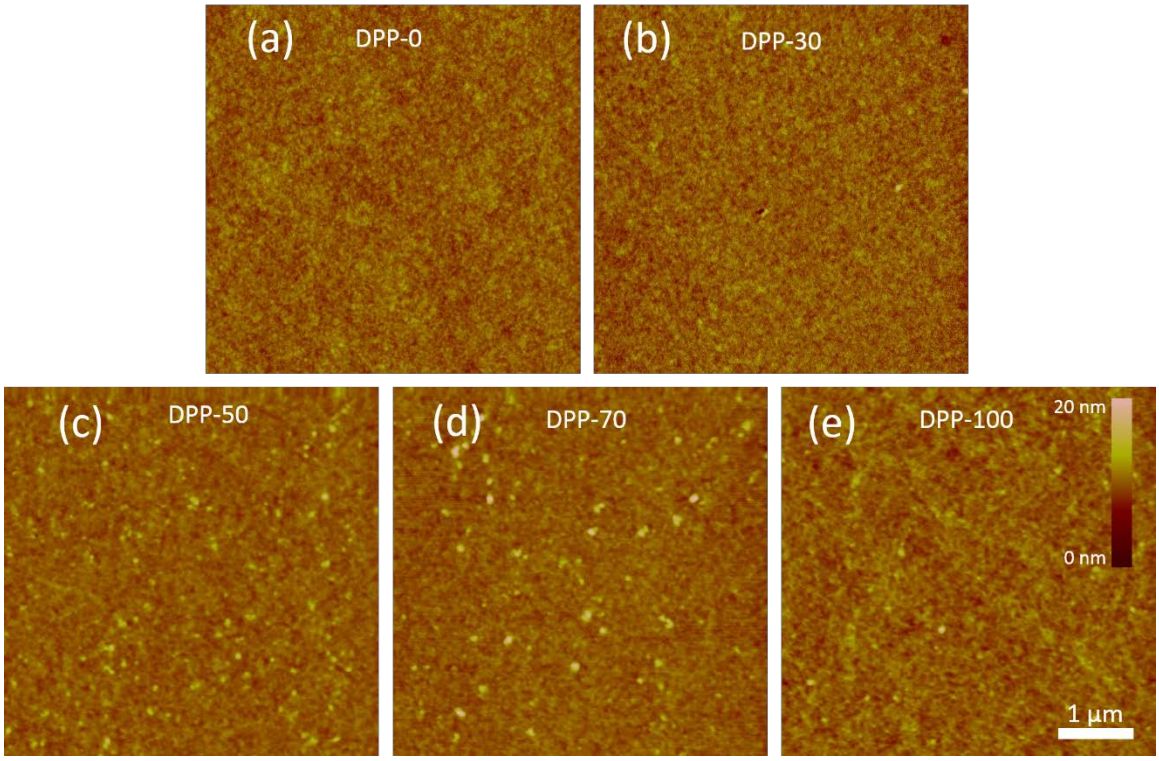

Fig. S11 AFM images of polymer thin films without annealing. The polymer thin films were fabricated by spin coating on OTS modified Si/SiO_2 substrates.

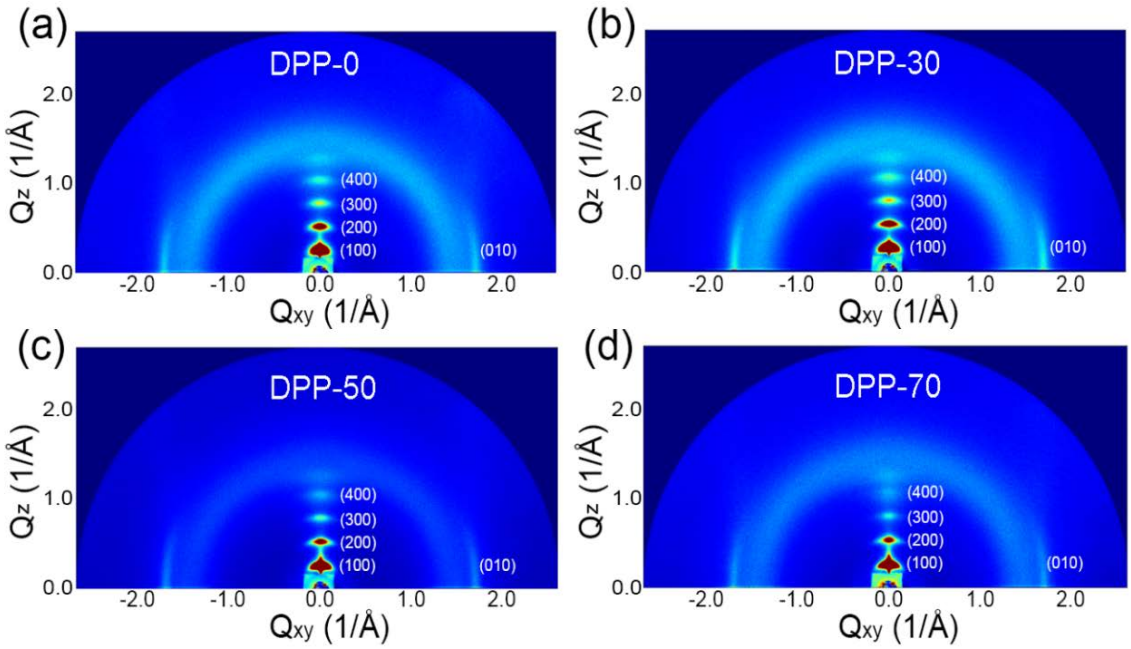

Fig. S12 2D-GIXRD patterns of DPP-0, 30, 50 and 70 thin films fabricated by spin coating on OTS modified wafer. The annealing temperature was 150 °C.

Downloaded from pubs.acs.org/mamobx/article-supplement/1550151/pdf/ma5b00194_si_001/ by PURDUE UNIV user on 28 October 2026

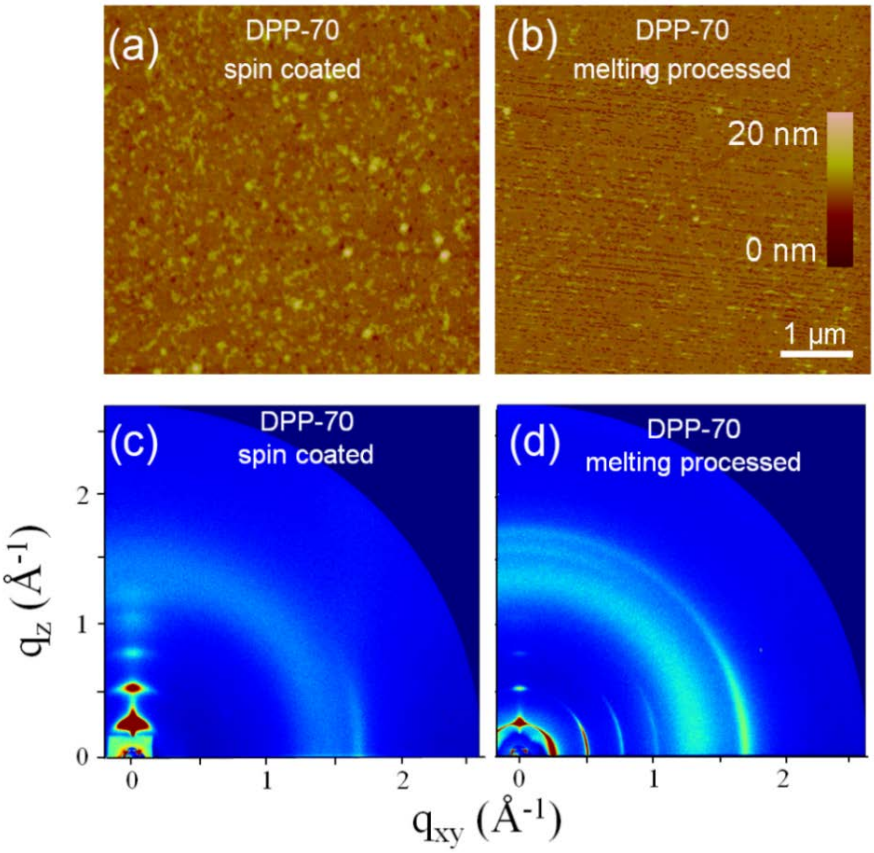

Fig. S13 (a) And (b) are AFM images for DPP-70 film fabricated by spin coating and melt processing, respectively. (c) And (d) are GIXRD patterns for DPP-70 film fabricated by spin coating and melting, respectively.

Table S5 Crystallographic parameters for the melt processed DPP Polymer Films

	Spin coated					**Melting processed**		
	DPP-0	DPP-30	DPP-50	DPP-70	DPP-100	DPP-70	DPP-100	
							peak 1	peak 2
lamella spacing (Å)	22.28	22.07	21.96	21.75	21.64	22.61	22.91	21.59
lamella peak FWHM (1/Å)	0.0436	0.0382	0.0387	0.0411	0.0345	0.0232	0.0123	0.0163
π- π stacking distance (Å)	3.62	3.64	3.65	3.65	3.62	3.64	3.64	
π- π peak FWHM (1/Å)	0.0844	0.0779	0.087	0.0758	0.063	0.0613	0.0578	

Downloaded from pubs.acs.org/mamobx/article-supplement/1550151/pdf/ma5b00194_si_001/ by PURDUE UNIV user on 28 October 2026